Additive manufacturing of nickel superalloys

Contents

- Introduction
- IN718
- IN625
- Hastelloy X
- Non-weldable nickel superalloys
- Design of new nickel superalloys

Introduction

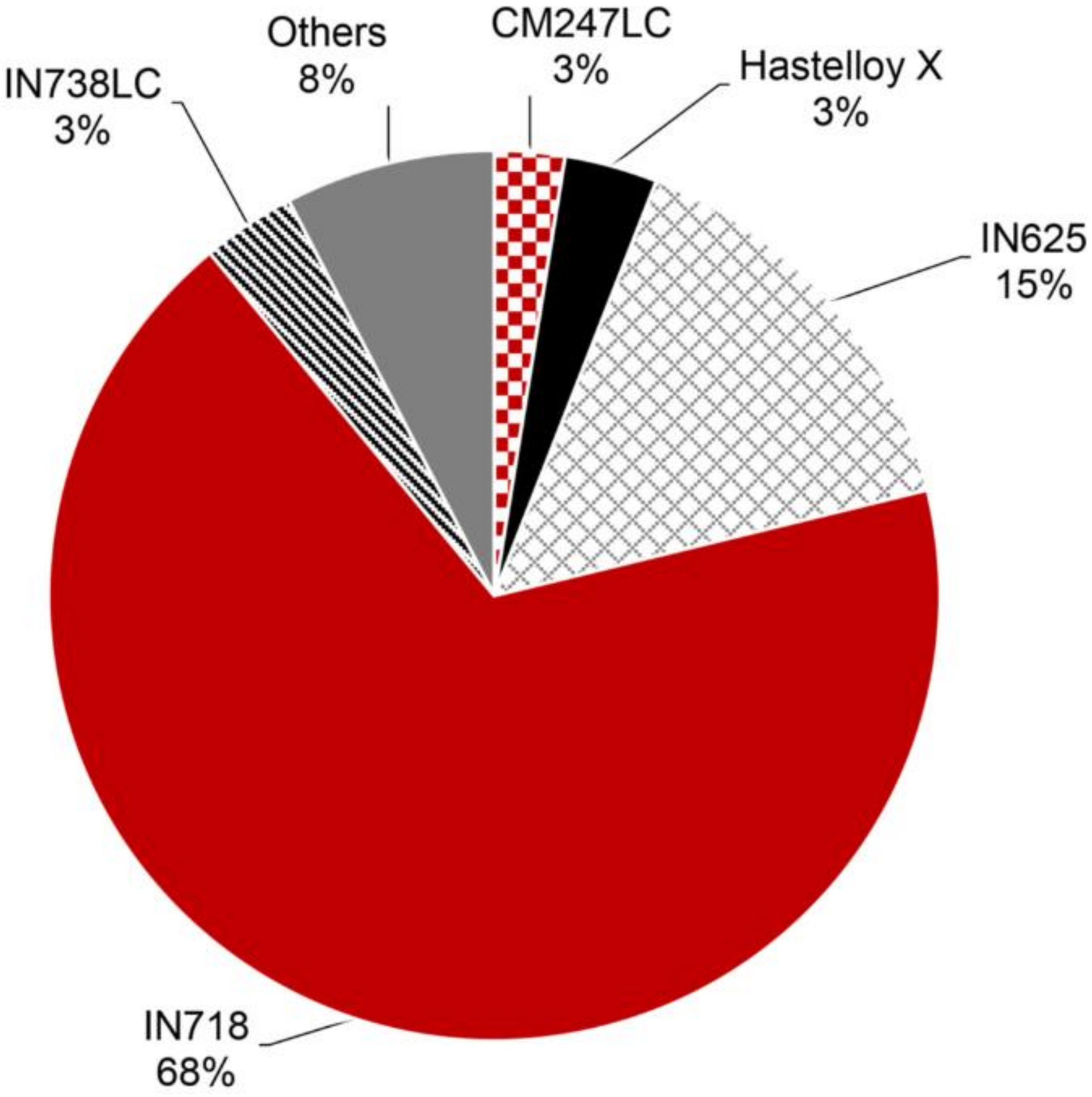

Fig. Research literature focus on nickel-based superalloys for powder-based AM

Source: Sanchez et al. 2021 [https://doi.org/10.1016/j.ijmachtools.2021.103729]

Introduction

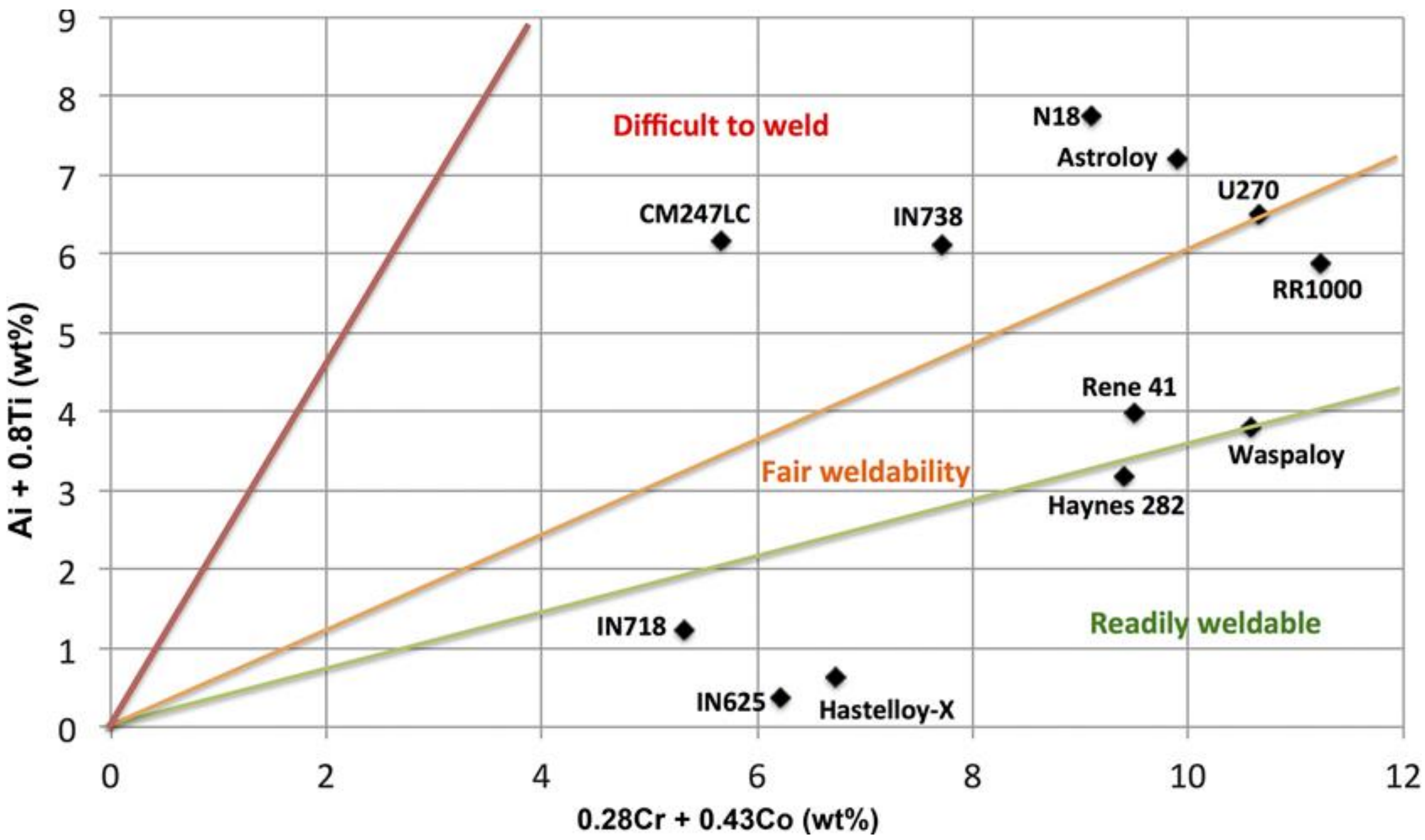

Fig. Diagrams of weldability of nickel-based superalloys based on their chemical composition

Source: Attallah et al. 2016 [https://doi.org/10.1557/mrs.2016.211]

Introduction

Table 1.1: The nominal composition of the most commonly AMed nickel superalloys. All compositions are in weight percent.

Alloy	Ni	Cr	Fe	Mo	Nb	Ta	Ti	Al	Co	Mn	Si	Cu	C	W	Hf	B	Zr
IN718	50-55	17-21	11-25	2.8-3.3	2.4-2.8	2.4-2.8	0.65-1.2	0.2-0.8	<0.1	<0.35	<0.35	<0.3	<0.08	-	-	-	-
IN625	58-69	20-23	<5	8-10	3-4	0.15	<0.4	<0.4	<1	<0.5	<0.5	-	<0.1	-	-	-	-
IN738LC	61.7	16	-	1.75	0.8	1.7	3.5	3.5	8.5	<0.04	-	-	0.1	2.6	-	-	-
CM247LC	61.7	8.1	-	0.5	-	3.2	0.7	5.6	9.2	-	-	-	0.07	9.5	1.4	0.015	0.015
Hastelloy X	47	22	18	9	0.5	-	0.15	0.5	1.5	1	1	-	0.1	0.6	-	0.008	-
Rene 80	Bal.	14.06	-	4.04	-	-	5.04	2.91	9.59	-	-	-	0.17	4.14	-	-	0.08
AM80	Bal.	14.1	-	3.82	-	2.43	2.86	3.22	9.67	-	-	-	0.15	4.19	1.05	-	0.04
WSU 150	Bal.	17.83	-	5.3	0.45	0.9	2.75	2.44	9.29	-	-	-	0.09	1.33	-	-	-
ABD-850AM	Bal.	18.68	-	1.89	0.6	0.44	2.22	1.29	17.6	-	-	-	0.01	4.74	-	0.003	-

IN718

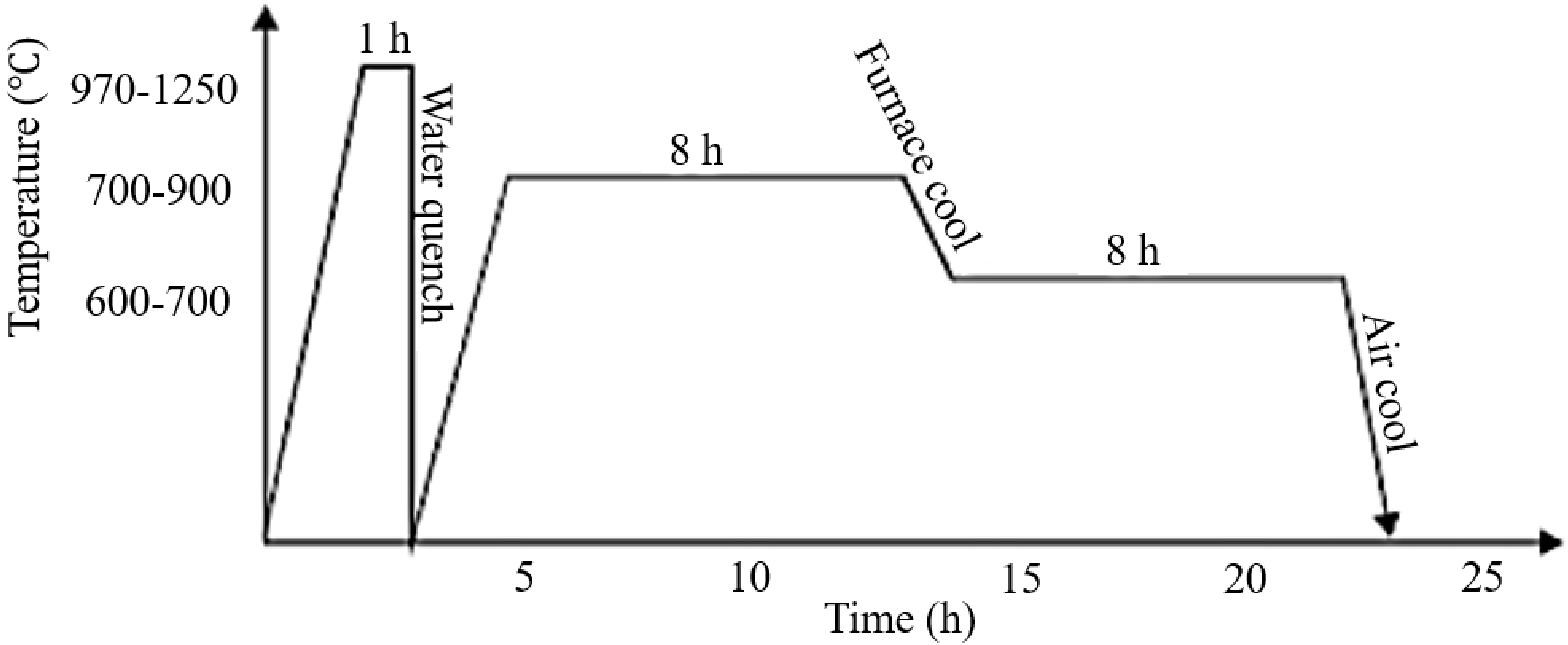

Fig. Schematics heat treatment procedure for IN718

IN718

Fig. (a) and (b) SEM micrographs of an LPBFed and stress relieved IN718 showing δ and Laves phase precipitates, (c) TEM bright field micrograph, showing various precipitate morphologies in the LPBFed and stress relieved IN718, and (d) Corresponding EDS analysis showing the presence of δ precipitates and carbides in the LPBFed and stress relieved IN718

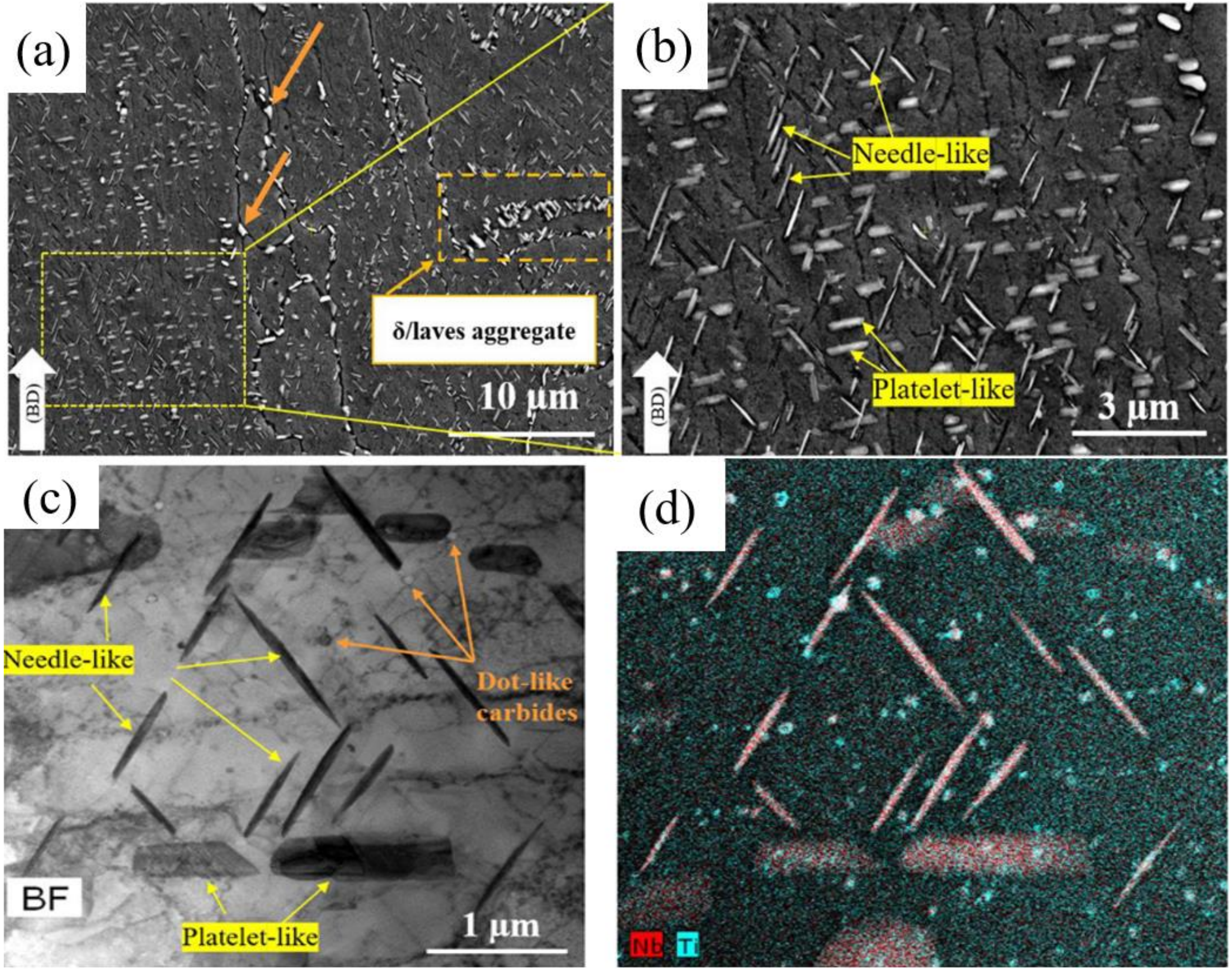

Source: Hasani et al. 2021 [https://doi.org/10.1016/j.matchar.2021.111499]

IN718

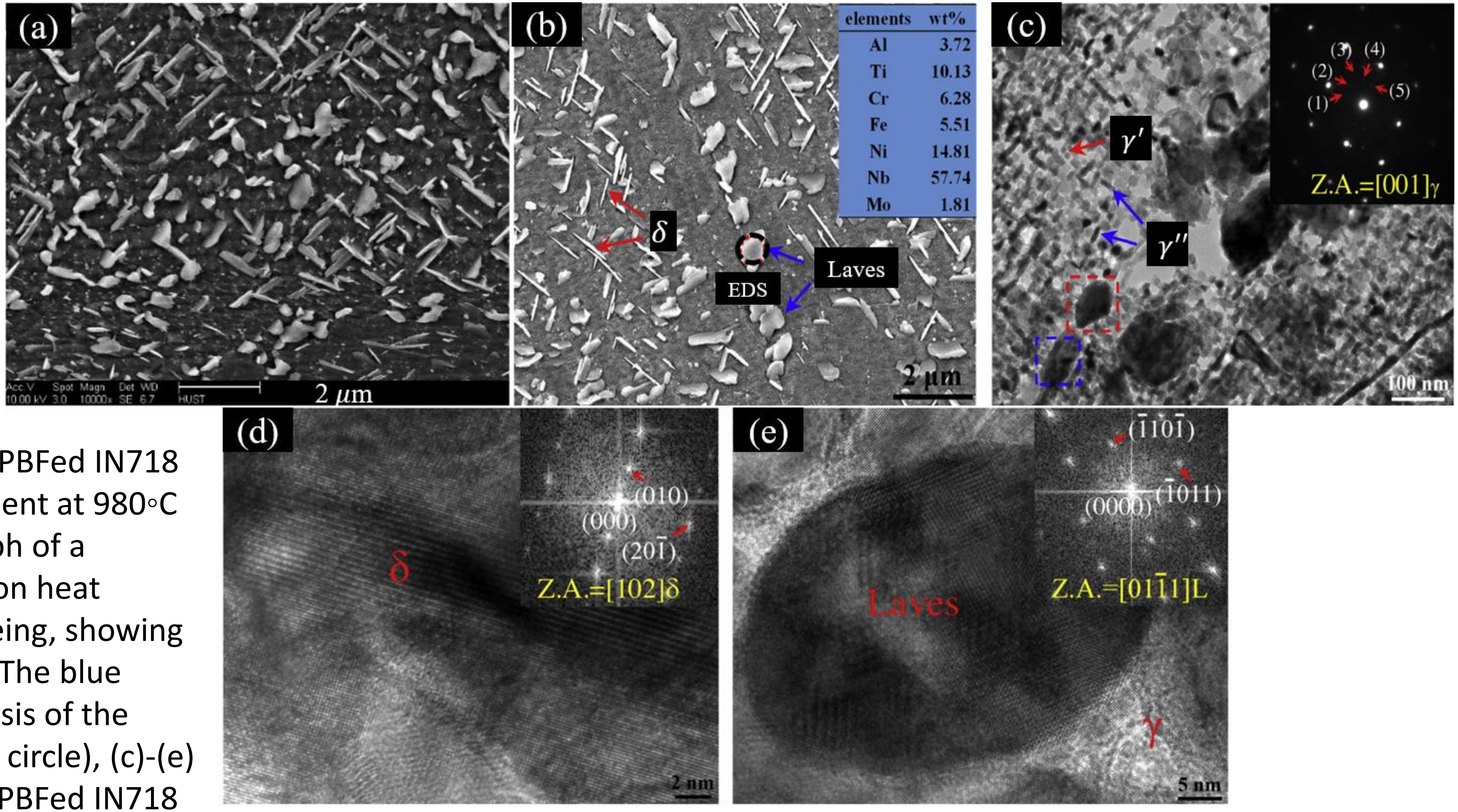

(a) SEM micrograph of a LPBFed IN718 after solution heat treatment at 980◦C for 1 h, (b) SEM micrograph of a LPBFed IN718 after solution heat treatment and double ageing, showing the residual Laves phase (The blue inset shows the EDS analysis of the region in the dotted black circle), (c)-(e) TEM micrographs of the LPBFed IN718 after solution heat treatment and double ageing, showing the presence of γ′, γ′′, δ and Laves precipitates

Source: Luo et al. 2020 [https://doi.org/10.1016/j.addma.2019.100875]

IN718

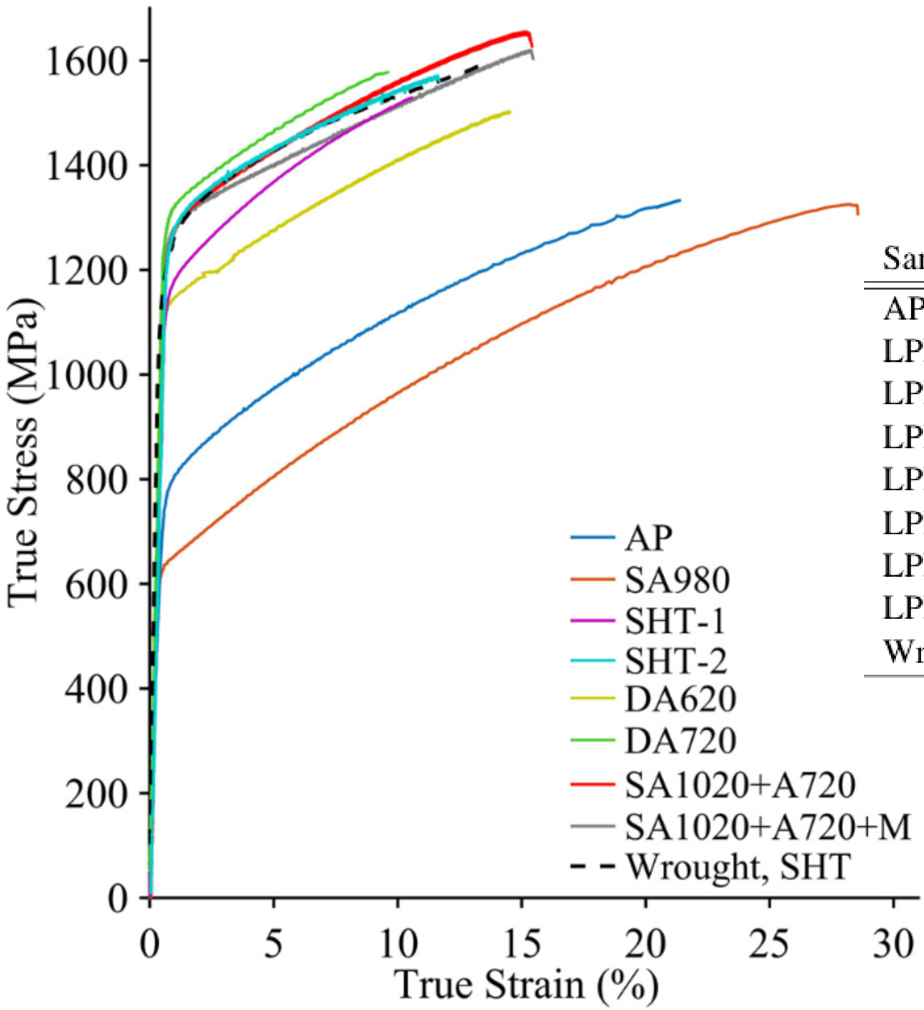

Fig. Tensile behaviour of LPBFed IN718 in the as-built state and after various heat treatments compared to a wrought and heat treated IN718

Table: Heat treatment schemes corresponding to mechanical testing results shown in Fig.

Sample	Solution annealing	Ageing
AP (LPBFed as-built)	-	-
LPBFed+SA980	980°C, 1 h, Water quench	-
LPBFed+SHT-1	980°C, 1 h, Air cooled	Double aged at 720°C and 620°C
LPBFed+SHT-2	980°C, 1 h, Air cooled	Machined and double aged at 720°C and 620°C
LPBFed+DA620	-	Directly aged at 620°C for 24 h, Air cooled
LPBFed+DA720	-	Directly aged at 720°C for 24 h, Air cooled
LPBFed+SA1020+A720	1020°C, 15 min, Water quench	720°C, 24 h, Air cooled
LPBFed+SA1020+A720+M	1020°C, 15 min, Water quench	Machined, 720°C, 24 h, Air cooled
Wrought, SHT	980°C, 1 h, Air cooled	Double aged at 720°C and 620°C

IN625

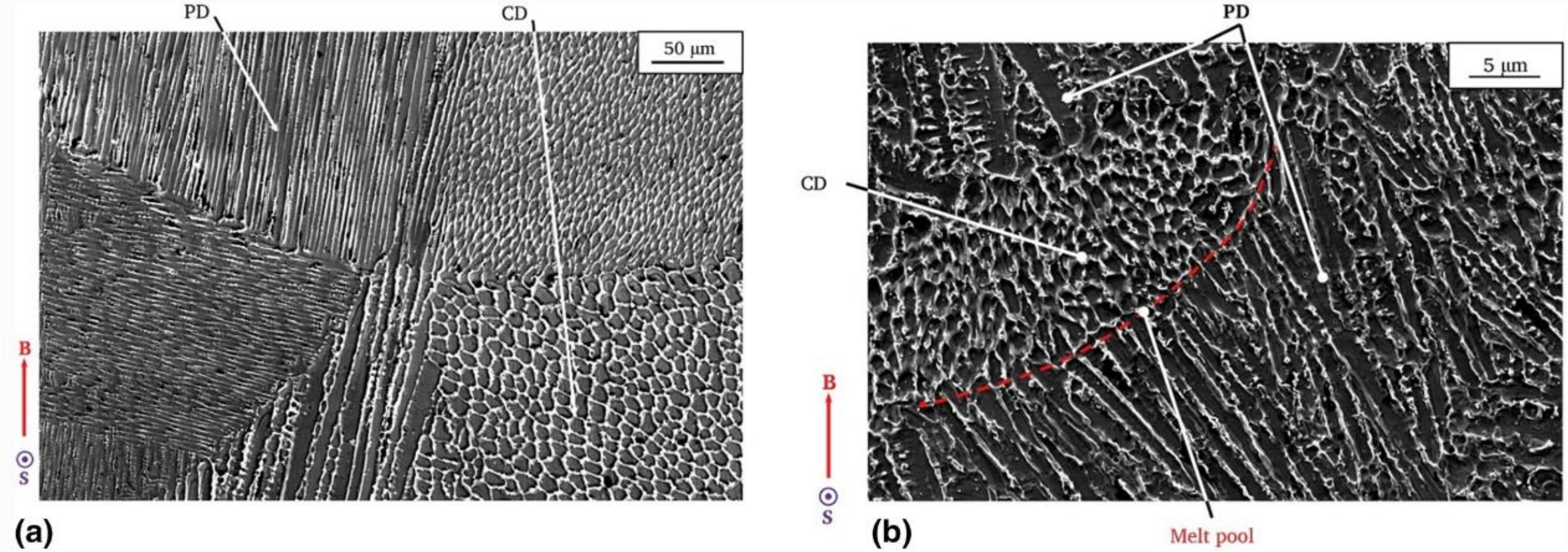

Fig. (a) SEM micrograph of an IN625 sample after LPBF (b) SEM micrograph of an IN625 sample after LMD (PD- Primary Dendrites; CD- Cell-like Dendrites; B- Building direction; S- Scanning direction)

Source: Karmuhilan, and Kumanan 2021 [https://doi.org/10.1007/s11665-021-06427-3]

IN625

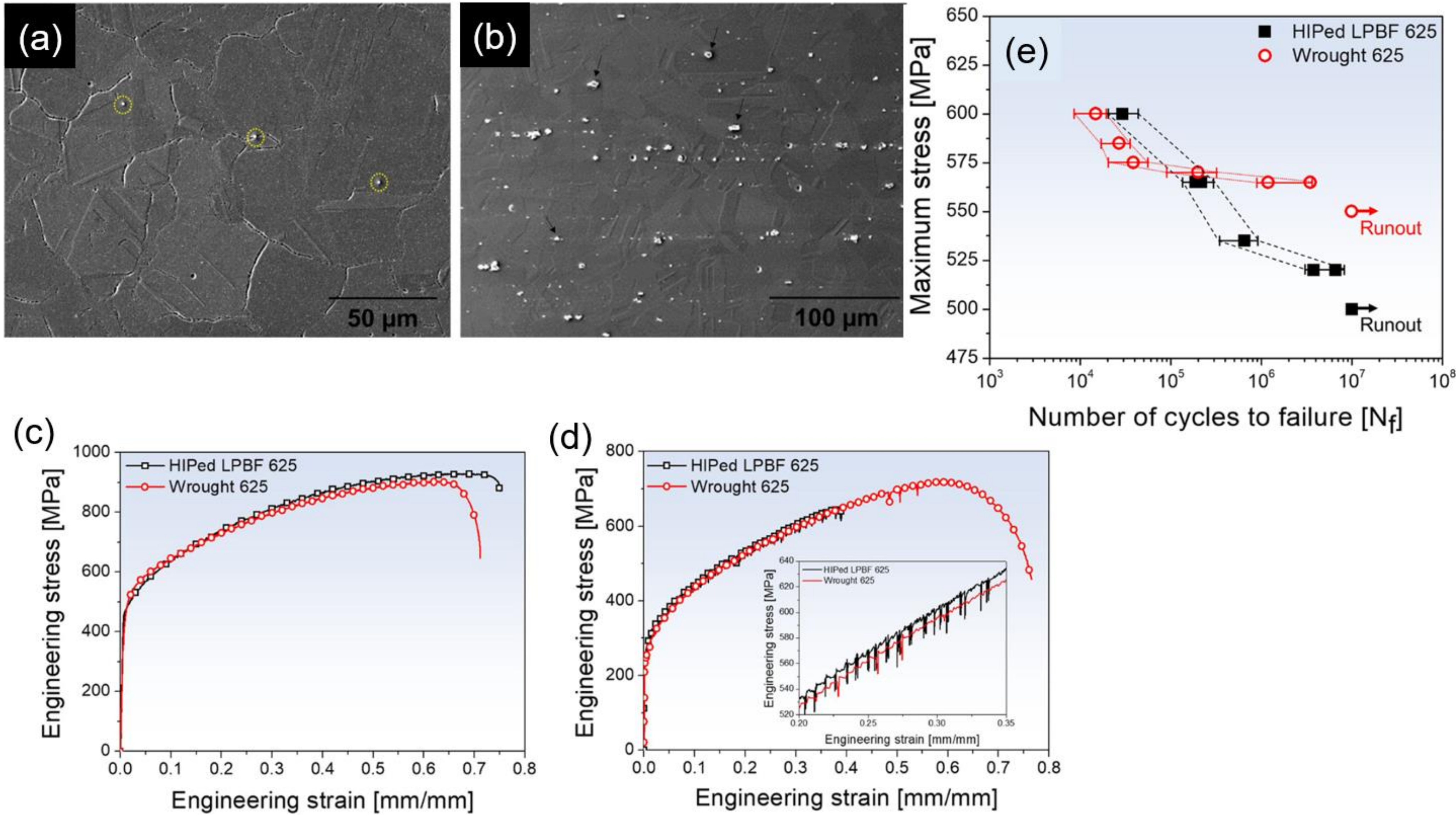

Fig. SEM micrographs showing typical (a) HIPed LPBF IN625 and (b) wrought IN625 microstructures (Yellow circles with dots and black arrows denote Al_2O_3 and carbides, respectively), (c) and (d) Tensile behaviour of HIPed LPBF IN625 and wrought IN625 at room temperature and 650◦C, respectively (Inserted graph shows the serrated flows of HIPed LPBF IN625 and wrought IN625), and (e) Maximum stress and fatigue life of HIPed LPBF IN625 and wrought IN625 at 650◦C

Source: Kim et al. 2020 [https://doi.org/10.1016/j.addma.2020.101377]

Hastelloy X

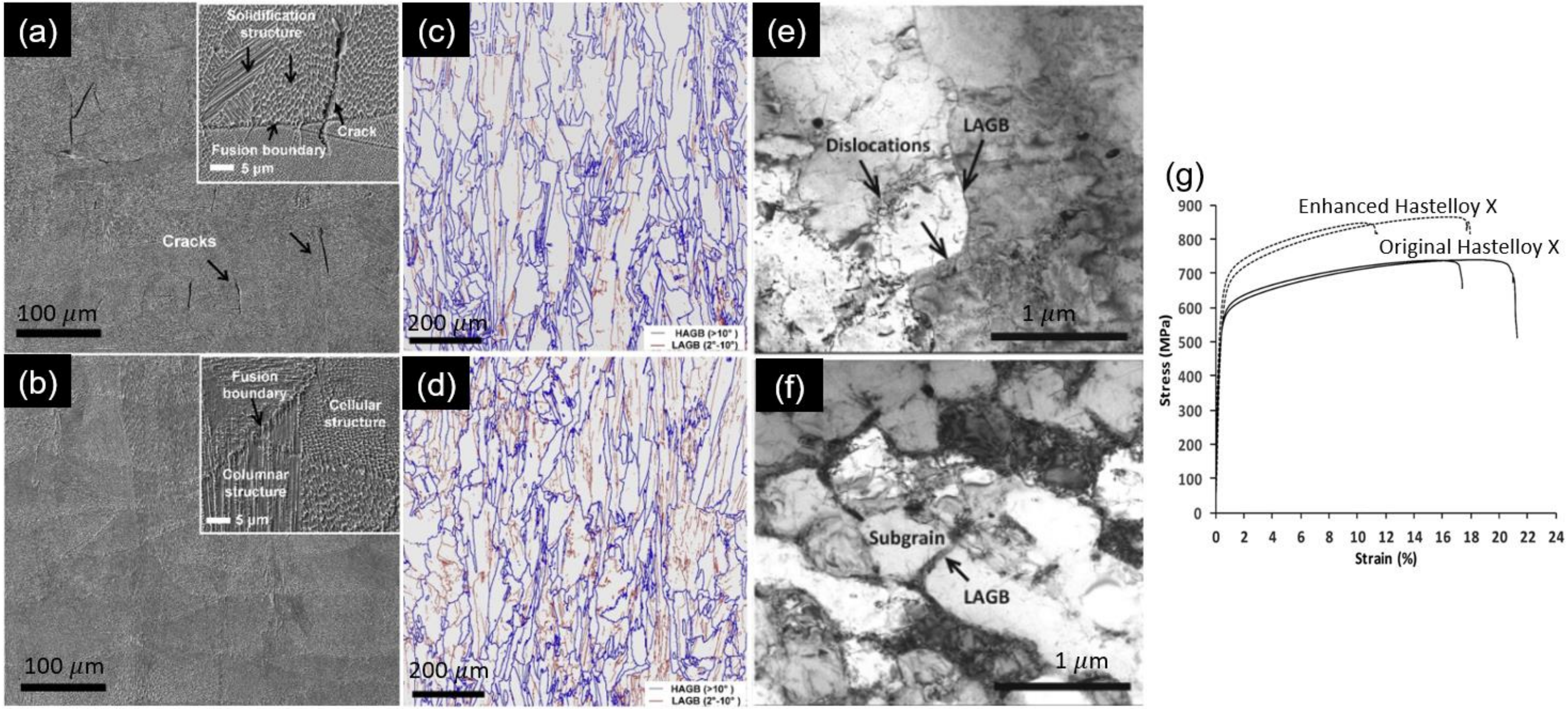

Fig. (a) and (b) Representative SEM micrographs of LPBFed original and enhanced Hastelloy X, respectively, revealing the columnar and cellular solidification structures, as well as cracks. (c) and (d) EBSD grain boundary maps showing the distribution of HAGBs (blue) and LAGBs (red) in the LPBFed original and enhanced Hastelloy X, respectively. (e) and (f) Bright field TEM micrographs of LPBFed original and enhanced Hastelloy X, respectively. (g) Tensile testing curves of LPBFed original and enhanced Hastelloy X

Source: Han et al. 2019 [https://doi.org/10.1016/j.addma.2019.100919]

Non-weldable nickel superalloys

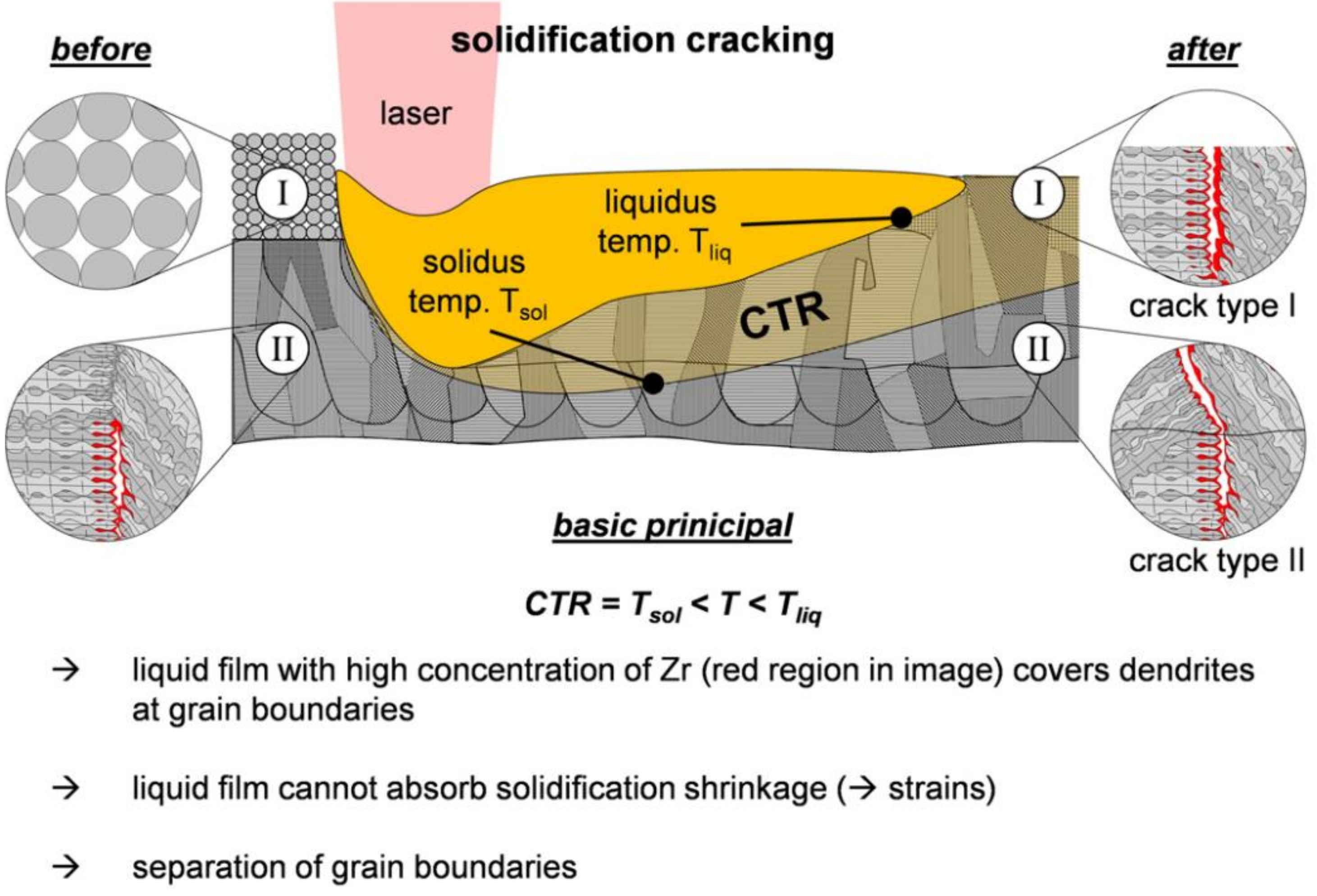

Fig. Schematics of solidification crack formation in LPBFed IN738LC

Source: Cloots et al. 2016 [https://doi.org/10.1016/j.matdes.2015.10.027]

Non-weldable nickel superalloys

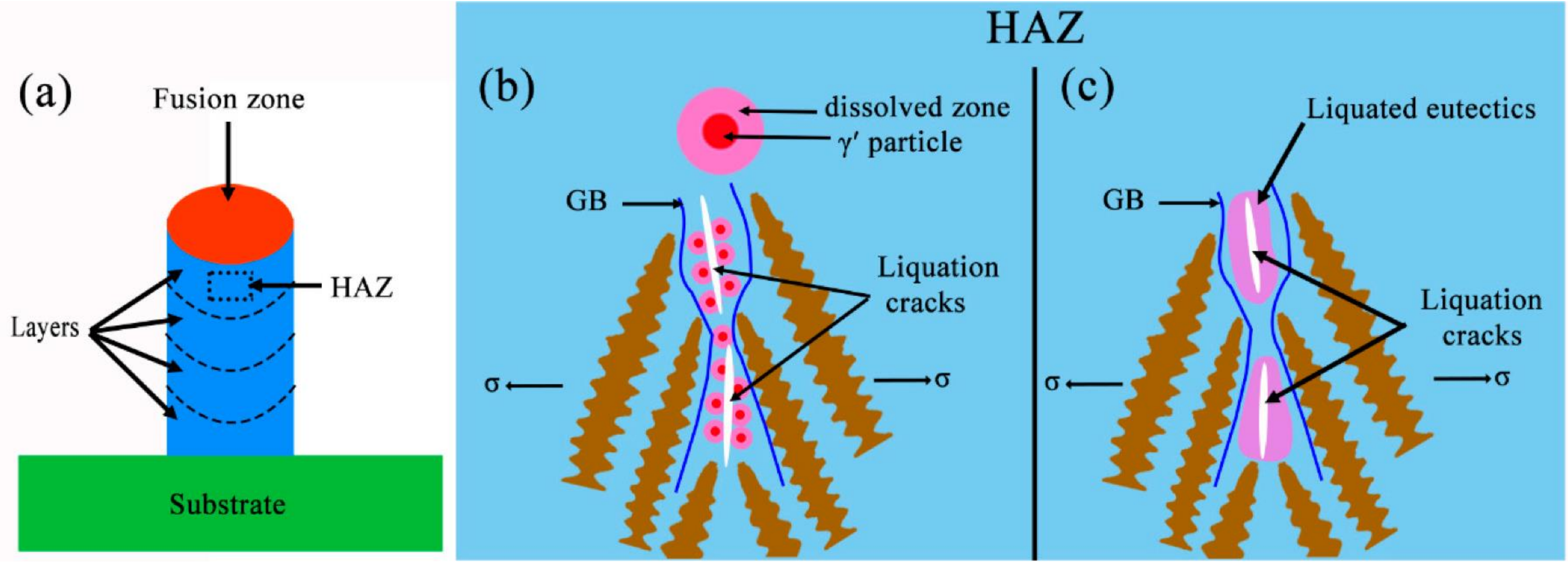

Fig. Schematic diagram showing the locations of (a) the heat-affected zone (HAZ), (b) constitutional liquation of γ′ particles, and (c) localised melting of γ–γ′ eutectics as two different liquation mechanisms in IN738LC (GB and σ are grain boundary and stress, respectively)

Source: Wang et al. 2020 [https://doi.org/10.3390/ma13183924]

Design of new nickel superalloys

- AMed Rene 80 is susceptible to cracking, limiting its adoption for gas turbine blades. The addition of Ta and Hf, and reduction in Ti contents from the original Rene 80 has led to the development of a new AM80 nickel superalloy that can be produced crack-free through EBM.
- In WSU 150, by successfully suppressing the precipitation kinetics, a novel nickel superalloy has been created using the combinatorial alloy design technique in conjunction with CALPHAD-based solidification Modelling.
- ABD-850AM is also designed for AM, which showed remarkable improvement in crack susceptibility compared to CM247LC alloy

Considerations to estimate crack susceptibility:

i. the solidification temperature range that can be obtained from a Scheil simulation of non-equilibrium solidification and assuming no back-diffusion;
ii. an estimate of the resistance to strain-age cracking during thermal cycling and post processing for each trial composition;
iii. calculation of high temperature yield stress; and
iv. creep resistance to guarantee functionality and stability